

Baric dependence of the Néel temperature of La_2CuO_4

V. D. Doroshev, V. N. Krivoruchko, M. M. Savosta, A. A. Shestakov,
and T. N. Tarasenko

A. A. Galkin Physico-Mechanical Institute at Donets, National Academy of Sciences of Ukraine,
340114 Donets, Ukraine

(Submitted 29 December 1995)

Zh. Eksp. Teor. Fiz. **110**, 943–958 (September 1996)

We have used nuclear quadrupole resonance (NQR) of ^{139}La nuclei to study the dependence of the Néel temperature of La_2CuO_4 on pressure in the range of hydrostatic pressures up 1.3 GPa. We have established that the magnetic ordering temperature increases with pressure at a rate $dT_N/dP = 7.8 \text{ K/GPa}$, and that the critical index β increases from a value of 0.26 at atmospheric pressure to a value of 0.31 at 1.3 GPa. The theoretical interpretation of our results is based on a quantum model of La_2CuO_4 using the spectral properties of the spin Green's functions. By comparing these theoretical calculations with the experimental results, we can establish how the system magnetic parameters depend on pressure. In particular, we have analyzed the dependence of the exchange and relativistic interactions of La_2CuO_4 on its crystal structure. © 1996 American Institute of Physics. [S1063-7761(96)01409-6]

1. INTRODUCTION

As is well known, copper-containing high- T_c materials have a layered structure with the CuO_2 planes as the fundamental crystallographic element. It is also well known (see, e.g., the reviews Refs. 1–4), that the magnetic moment of the copper Cu^{2+} ions in these planes turns out to have a considerable effect on the motion of charge carriers, which are present when the original (base) compounds are suitably doped: R_2CuO_4 , $\text{RBa}_2\text{Cu}_3\text{O}_8$, RBa_4CuO_8 , $\text{La}_2(\text{Ca},\text{Sr})\text{Cu}_2\text{O}_8$, and $\text{Bi}_2\text{Sr}_2\text{CaCuO}_8$, where R is a rare-earth element. For this reason, the magnetic and superconducting properties of copper-containing high- T_c superconductors are closely related to one another. Thus, for example, a proportional dependence is observed between the magnetic ordering temperature T_N for the copper spins of the base compound and the maximum superconducting transition temperature T_c for the corresponding superconducting material.⁴ Thus, the increasing interest shown by researchers in the magnetism of high- T_c superconductors is not surprising.

The orthorhombic antiferromagnets $\text{La}_2\text{CuO}_{4+\delta}$ present unique opportunities for investigating the interrelations between the magnetic, transport, and structural properties of high- T_c superconductors. The compound $\text{La}_2\text{CuO}_{4+\delta}$, which is the base for the class of compounds $\text{La}_{2-x}(\text{Ba},\text{Sr})_x\text{CuO}_{4-y}$ with “hole” type superconductivity, undergoes magnetic and superconducting transitions in combination with orthorhombic–tetragonal structural phase transformations, depending on the content of excess oxygen δ . For example, a value of $T_c \approx 40 \text{ K}$ is observed in samples with the value $\delta \approx 0.13$. At the same time, the value of δ also controls the magnetic ordering temperature T_N . For example, in compounds synthesized at high pressure, for $\delta \approx 0.13$ we have $T_N \rightarrow 0 \text{ K}$, whereas in samples synthesized in air, $T_N \approx (220\text{--}250) \text{ K}$; the maximum value $T_N \approx 325 \text{ K}$ is recorded in essentially stoichiometric crystals with respect to oxygen ($\delta = 0$) that have been thermally processed in a vacuum or an inert gas.⁴

As for structural properties, at low temperatures and normal pressures the crystal lattice of $\text{La}_2\text{CuO}_{4+\delta}$ is orthorhombic, with space symmetry group C_{mca} . For stoichiometric samples an orthorhombic–tetragonal transition $C_{mca} \leftrightarrow I4/mmm$ takes place at $T \sim 550 \text{ K}$ (normal pressure);⁵ changing δ significantly affects the temperature of this transformation.⁶

It is well known that external hydrostatic pressure strongly affects the structural orthorhombic–tetragonal transition in $\text{La}_2\text{CuO}_{4+\delta}$, stabilizing the tetragonal phase. Thus, the tetragonal phase is induced at room temperature by a moderate pressure $P \approx 3.6 \text{ GPa}$.⁵ There exist detailed studies of the structural parameters of this compound as a function of pressure (see, e.g., Refs. 5–8 and review Ref. 9), a circumstance that is important from the point of view of establishing and further interpreting results of high-pressure experiments.

Nevertheless, existing data in the literature on the pressure dependence of the magnetic properties of $\text{La}_2\text{CuO}_{4+\delta}$ are quite contradictory. Thus, in previous investigations a variety of measurements have been made on the baric coefficient $(1/T_N)(dT_N/dP)$ both by indirect methods (based on anomalies in the magnetic susceptibility and conductivity^{10–12}) and direct methods (neutron diffraction¹³). The goal of these investigations was to test a number of “magnetic” models of high- T_c superconductors by comparing the value of $(1/T_N)(dT_N/dP)$ for weakly doped material with the value of the baric coefficient of the superconducting transition temperature $(1/T_c)(dT_c/dP)$ for superconducting (doped) compounds. The values of the coefficient $(1/T_N) \times (dT_N/dP)$ obtained in Refs. 10–13 for $\text{La}_2\text{CuO}_{4+\delta}$ are not only characterized by a large scatter but even differ in sign.

In our view, the unreliability of the results of these investigations can be explained as follows. In these papers the authors did not take into account the phenomenon of fluctuation-induced disruption of the continuous second-order magnetic phase transition, which converts it to a dis-

continuous first-order transition, an effect that was discovered later.^{14,15} Nuclear resonance investigations based on nuclear quadrupole resonance (NQR)¹⁴ and nuclear gamma resonance (NGR) methods¹⁶ have shown that near T_N in $\text{La}_2\text{CuO}_{4+\delta}$ is in a heterogeneous state as a result of the coexistence of antiferromagnetic and paramagnetic phases over a rather wide range of temperatures; the volumes of these phases readjust smoothly as the temperature ranges over the critical region. We note that the temperature hysteresis phenomena observed in Refs. 12, 17 provide indirect confirmation of the existence of a first-order magnetic phase transition in $\text{La}_2\text{CuO}_{4+\delta}$. However, the authors of Ref. 12 assumed that this was caused by stratification of phases that differ in oxygen content. We also note that the measurements of $(1/T_N)(dT_N/dP)$ reported in Refs. 10–13 were made using crystals with low values of T_N in the range 200 to 260 K, i.e., with a large excess oxygen content, and consequently a large carrier concentration. This factor complicates the interpretation of their results, due to the frustration of the magnetic interactions.¹⁸

With the goal of clarifying the complexities of the present-day experimental situation, we have carried out a detailed investigation of the effect of hydrostatic compression on the critical behavior of antiferromagnetic $\text{La}_2\text{CuO}_{4+\delta}$. To accomplish this, we have used a noninvasive method with high information content: NQR of ^{139}La . Because this technique is local, it allows us to separately record the signals of the antiferromagnetic and paramagnetic phases. The high information yield of ^{139}La NQR in investigating the magnetic properties of $\text{La}_2\text{CuO}_{4+\delta}$ was demonstrated previously, for example, in Refs. 19–24. Once we have eliminated the uncertainty caused by phase coexistence, we can accurately reproduce the temperature dependence of the sublattice magnetizations both at normal and high (~ 1.3 GPa) pressures. In order to eliminate uncertainties connected with superstoichiometric oxygen, we studied samples with a high value of T_N , i.e., close to stoichiometric in content. Since these samples are magnetic insulators, the theoretical interpretation of our results becomes easier.

The theoretical interpretation of our results is based on a quantum Heisenberg model for La_2CuO_4 .^{23,25} Using the spectral properties of spin Green's functions (calculated in the random phase approximation), we obtain a general expression for the Néel temperature T_N . Existing data on the baric dependence of several structural and magnetic parameters of $\text{La}_2\text{CuO}_{4+\delta}$ allows us to establish with reasonable certainty the nature of the pressure dependence of the system magnetic parameters. We examine the role of the exchange and relativistic interactions in establishing the critical properties of the system. In particular we show that, contrary to the conclusions of previous papers, $\text{La}_2\text{CuO}_{4+\delta}$ remains magnetically ordered both in the tetragonal and orthorhombic phases.

2. EXPERIMENT

1. Methodology

Nuclear resonance studies of the critical behavior of antiferromagnetic $\text{La}_2\text{CuO}_{4+\delta}$ at normal and high pressures are

noninvasive since they do not require the introduction of impurities as probes, nor the imposition of an external magnetic field. Investigations based on the method of nuclear magnetic resonance (NMR) directly record the local fields at $^{63,65}\text{Cu}$ nuclei of the magnetoactive Cu^{2+} ions. This method is fairly direct; unfortunately, it cannot be implemented due to the rapid decrease of the characteristic spin–spin relaxation time T_2 with temperature.²⁶

An approach that turns out to be very productive is to use ^{139}La nuclei as natural probes ($I=7/2$, $\gamma/2\pi=601.44$ Hz/Oe, $Q=0.21$ b) of the nominally diamagnetic La^{3+} ions present in the structure of $\text{La}_2\text{CuO}_{4+\delta}$. In this case, the temperature dependence of the reduced sublattice magnetization $M(T)/M(0)$ can be extracted from the value of the local fields \mathbf{H}_{loc} (dipole and indirect hyperfine) generated at the ^{139}La nuclei by the surrounding Cu^{2+} ions. The moments μ_{Cu} of these ions are in turn measured by NQR. For direct NQR of ^{139}La the value of T_2 is large up to the temperature T_N , and the narrowness of the NQR spectral lines make high-precision measurements of $M(T)/M(0)$ feasible. Although this method is more indirect, estimates show that the systematic errors originating from the thermal expansion of the crystal and the change in the degree of orthorhombic character with temperature do not exceed 1 to 2%.²³

In interpreting the NQR spectra of ^{139}La so as to obtain values of \mathbf{H}_{loc} it is necessary to take into account the following factors. In the low-symmetry orthorhombic structure C_{mca} ($a < c < b$), the La^{3+} ions occupy the $(8f)$ position with point group $m=\bar{2}$. Because of this, the electric field gradient tensor at the nucleus is not axial; however, the analysis data reported in Ref. 27, combined with the use of direct numerical diagonalization of the nuclear spin Hamiltonian to interpret the spectra,¹⁹ reveal that even at low (helium) temperatures the asymmetry factor for the electric field gradient $\eta=(v_{yy}-v_{xx})/v_{zz}$ does not exceed a small value (0.01 ± 0.01). For this reason, in interpreting our spectra we can assume that the electric field gradient is axially symmetric ($\eta=0$). As the temperature increases to $T=T_N$ and as the pressure increases, the value of η should become still smaller due to the decrease in the orthorhombic distortion, since the orthorhombic–tetragonal transformation $C_{mca} \leftrightarrow I4/mmm$ takes place at temperatures and pressures comparable to our experimental conditions.

The theory of the NQR spectrum of ^{139}La in $\text{La}_2\text{CuO}_{4+\delta}$ has been the subject of a large number of papers.^{19–21,27} The complex structure of the spectrum is determined by the simultaneous interaction of the quadrupolar moment of the nucleus with the electric field gradient and its magnetic moment with the field \mathbf{H}_{loc} . In the paramagnetic phase of $\text{La}_2\text{CuO}_{4+\delta}$ ($\mathbf{H}_{\text{loc}}=0$) we can induce three different transitions with $\Delta m=1$ between the four degenerate quadrupole levels with $m=\pm 7/2, \dots, \pm 1/2$ at frequencies which for axial symmetry of the electric field gradient satisfy the relations

$$\nu_{3/2 \leftrightarrow 1/2} = (1/2) \nu_{5/2 \leftrightarrow 3/2} = (1/3) \nu_{7/2 \leftrightarrow 5/2} = \nu_Q \\ = (1/14h)eQv_{zz}. \quad (1)$$

The asymmetry of the electric field gradient tensor does not

lift the degeneracy of the levels, i.e., it does not change the number of lines, but it can change the frequency ratios (1) somewhat.²⁸

In the antiferromagnetic phase of $\text{La}_2\text{CuO}_{4+\delta}$, the NQR spectrum of ^{139}La has a more complicated structure consisting of nine lines measured over a wide range of frequencies from 2 to 20 MHz. It was reliably determined in Refs. 19, 29 that at low temperatures, in agreement with the crystal symmetry, the field \mathbf{H}_{loc} that causes the Zeeman splitting of the quadrupole levels lies in the bc -plane ($\phi=0$) at an angle $\theta \approx 78^\circ$ to the principal axis z of the electric field gradient tensor lying in this plane. In this geometry, the component $H_{\parallel} = H_{\text{loc}} \cos \theta$ parallel to the z axis turns out to be small ($\approx 0.2H_{\text{loc}}$) while the perpendicular component is decisive ($H_{\perp} = H_{\text{loc}} \sin \theta = 0.98H_{\text{loc}}$). In all known papers, two pairs of very intense high-frequency lines $\nu_5 - \nu_6$ and $\nu_7 - \nu_8$ are used to measure the reduced magnetization (using the notation of Ref. 21). These lines correspond to the transitions $7/2 \rightarrow 5/2$ and $5/2 \rightarrow 3/2$, at frequencies from 12 to 20 MHz. The splittings ($\nu_8 - \nu_7$) and ($\nu_6 - \nu_5$) are determined only by the component H_{\parallel} , which strongly reduces the accuracy of the measurements due to the smallness of the latter, and also leads to systematic errors due to the variation of θ with temperature. In order to increase the accuracy of our measurements, we measured the frequencies of the weak lines ν_1 to ν_4 for allowed and “forbidden” transitions $\pm 3/2 \rightarrow \Phi_{\pm 1/2}$ between states with $m = \pm 3/2$ and the mixed states $\Phi_{\pm 1/2}$ in the frequency range 5 to 8 MHz.¹⁹

Although the detection of these lines is more complicated, especially near T_N , the advantages of this approach are obvious. To first order in perturbation theory the formulas for the NQR frequencies of the lines $\nu_1 - \nu_4$ for an axially symmetric electric field gradient can be written as follows:³⁰

$$\begin{aligned} \nu_{1,2} &= \nu_{3/2 \leftrightarrow 1/2} \mp \frac{3}{2} \frac{\gamma}{2\pi} H_{\parallel} - \frac{1}{2} \frac{\gamma}{2\pi} \sqrt{H_{\parallel}^2 + (4H_{\perp})^2}, \\ \nu_{3,4} &= \nu_{3/2 \leftrightarrow 1/2} \mp \frac{3}{2} \frac{\gamma}{2\pi} H_{\parallel} + \frac{1}{2} \frac{\gamma}{2\pi} \sqrt{H_{\parallel}^2 + (4H_{\perp})^2}. \end{aligned} \quad (2)$$

Consequently, the splittings ($\nu_3 - \nu_1$) and ($\nu_4 - \nu_2$) are caused not so much by the component H_{\parallel} as by the AC component H_{\perp} . This fact allows us to improve the accuracy of our measurement of $H_{\text{loc}} = \sqrt{H_{\parallel}^2 + H_{\perp}^2}$ by almost an order of magnitude. Furthermore, by simultaneously including H_{\parallel} and H_{\perp} , we can eliminate systematic errors that arise from the changes in the degree of orthorhombic character with pressure and temperature. In order to average the frequencies of all the lines ν_1 to ν_4 , we define the components of H_{loc} themselves as follows:

$$\begin{aligned} \frac{\gamma}{2\pi} H_{\parallel} &= \frac{\nu_4 - \nu_3 + \nu_2 - \nu_1}{6}, \\ \frac{\gamma}{2\pi} \sqrt{H_{\parallel}^2 + (4H_{\perp})^2} &= \frac{\nu_4 + \nu_3 - \nu_2 - \nu_1}{2}. \end{aligned} \quad (3)$$

Note that the use of functions (2) and (3) to define the AC component H_{\perp} is entirely equivalent to the method described in Ref. 27.

2. Samples and apparatus

In these measurements we used a polycrystalline sample of $\text{La}_2\text{CuO}_{4+\delta}$, which was synthesized by starting with the oxides La_2O_3 and CuO and using ceramic technology. A preliminary anneal was carried out at 900°C for 20 hours, followed by grinding and pressing and then by a final anneal at 1100°C for 20 hours. After synthesis the sample was thermally processed in a vacuum of $\sim 10^{-2}$ Torr at 900°C for 12 hours. A strong narrowing of the NQR line and an increase in T_N from its value of ~ 260 K for a sample synthesized in air up to a value ~ 320 K after thermal processing indicated a decreased content of superstoichiometric oxygen.

The NQR spectrum was recorded by the Hahn two-pulse method with analog integration and recording in the course of a linear sweep of the oscillator frequency. In order to increase the accuracy of the resonance frequency measurements at fixed temperature and pressure, we recorded the spectra several times and then subjected the data to statistical processing on a computer. The errors in measuring the frequency were estimated to be $\pm(5-12)$ kHz depending on the temperature and pressure.

High pressures up to 1.3 GPa were created in a steel chamber of cylinder–piston type with a channel diameter of 11 mm, equipped with low-capacitance, high-voltage electric leads. The medium that transferred the pressure was polyethylsiloxane PES-5. The pressure in the chamber was measured with a manganin manometer. The temperature in the chamber was regulated by a gas-flow thermostat with a thermal carrier of cooled or heated nitrogen. The temperature was measured using a copper-constantan thermocouple. The sample was crushed and blended with outgassed paraffin in order to prevent degradation and to decrease the influence of pores on the uniformity of the pressure. A description of the high-pressure chamber was given in Ref. 31.

3. Measurement results

Measurements of the temperature dependences of the sublattice magnetizations were made at normal pressure and at a pressure $P = (1.27 \pm 0.07)$ GPa in the temperature range (4.2–325) K. The high-temperature portions of the experimental functions $M(T)/M(0) = H_{\text{loc}}(T)/H_{\text{loc}}(0)$ corresponding to the critical region are shown in Fig. 1 by dots. These measurements completely confirm the conclusions of Ref. 14 regarding the occurrence of a weak first-order phase transition in $\text{La}_2\text{CuO}_{4+\delta}$, both at normal and high pressures. Whereas at low temperatures the intensities of the lines ν_1 to ν_4 vary approximately as $1/T$, and are subject to the Boltzmann law, as the critical point is approached they begin to decrease abruptly without any significant line broadening or decrease in the transverse relaxation time T_2 . This behavior of the intensity indicates a rapid decrease in the volume of the antiferromagnetic phase as the temperature increases in the critical region. Signals from this phase become unobservable at approximately the same values of the reduced magnetization $M(T)/M(0) \approx 0.4$, both at normal and at high pressures. The corresponding temperature T_k at which the second-order transition collapses is to some degree arbitrary, since it depends on the ultimate measurable value of the

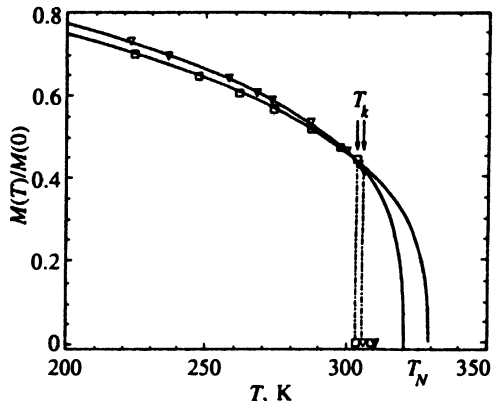


FIG. 1. Experimental (dots) and theoretical (curves) temperature dependences of the sublattice magnetizations of La_2CuO_4 in the vicinity of the magnetic ordering temperature for normal (∇) and high (\square) pressures (1.27 ± 0.07) GPa. The experimental results were approximated using Eq. (4). The arrows indicate the temperatures where the second-order phase transition collapses.

volume of antiferromagnetic phase. As is clear from Fig. 1, for the sample under study and identical sensitivities of the spectrometer we obtain $T_k \approx 306$ K at normal pressure and 303 K at high pressure, i.e., based on an ultimately measurable value of the antiferromagnetic phase volume of $\sim (0.05-0.1)$, the first-order phase transition temperature decreases with increasing pressure. As the temperature increases, starting from a value somewhat below T_k the signal intensity from the paramagnetic phase begins to increase abruptly, especially for the single line at frequency $\nu_{3/2 \rightarrow 1/2}$. The dependence of the intensity of this line on temperature saturates at $T = T_k + 5$ K. Consequently, in the critical region there is a transfer of “intensity” between the signals from the antiferromagnetic and paramagnetic phases, indicating a smooth redistribution of their volumes. This behavior is characteristic for a washed-out spatially nonuniform first-order phase transition. If a washed-out continuous transition were to occur (a second-order transition), we would observe “washing out” of the lines ν_1 to ν_4 near T_k over the entire frequency range from ν_1 to ν_4 due to the spatial distribution of values of sublattice magnetization and the fields H_{loc} corresponding to them. However, as we have already noted, this phenomenon does not occur. Measurements made while the temperature is increasing and decreasing do not reveal any hysteresis in the order-disorder transition, which is an indication of efficient seed formation.

Note that the normal-pressure data shown in Fig. 1 differ from those of Ref. 14 in that they indicate a wide interval of coexistence of the antiferromagnetic and paramagnetic phases; they also disagree on the value of the discontinuity in magnetization. Thus, in Ref. 14 the authors recorded a range of temperatures where the sample was heterogeneous of around 10 K, and a jump in reduced magnetization of ~ 0.33 . In contrast, our investigations show that the temperature interval for coexistence of the phases does not exceed 3 K, and that the jump in magnetization is ~ 0.4 . These quantitative differences are not fundamental, and arise, as we said above, from the arbitrary nature of the temperature T_k at

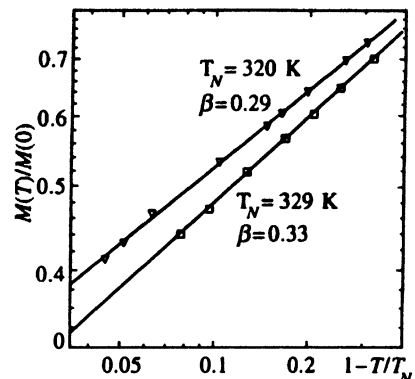


FIG. 2. Power-law fits to the temperature dependence of the sublattice magnetizations at normal and high pressures. The notation is the same as in Fig. 1. The values of T_N and β are presented for approximations in the temperature interval 220–306 K.

which the second-order transition collapses and we begin to detect a signal from the paramagnetic phase, which depends on the sensitivity of the spectrometer in the specific experiment. In the present study, our normal-pressure measurements were made on a sample placed in an unloaded high-pressure container. The resulting unavoidable decrease in the Q-factor of the input circuit appreciably degraded the sensitivity of the spectrometer compared to measurements without the container, which also leads to the apparent lack of agreement discussed above. Control measurements on a “free sample” demonstrate behavior in the critical region that coincides with that reported in Ref. 14.

Thus, a direct measurement of the value of T_N for $\text{La}_2\text{CuO}_{4+\delta}$ based on reducing the sublattice magnetization to zero ($M(T_N) = 0$) is impossible. In order to determine the Néel temperature and study the effect of hydrostatic pressure on it, we had to use an extrapolation procedure. We assumed that the behavior of $M(T)/M(0)$ in the critical region near T_N follows a power law:

$$M(T)/M(0) = D(1 - T/T_N)^\beta, \quad (4)$$

which is characteristic of second-order magnetic phase transitions. If approximation (4) adequately describes the experimental function $M(T)/M(0)$ in the range of temperatures below T_k , then the value of T_N can be obtained by extrapolating Eq. (4) to the range of temperatures above T_k until $M(T_N)/M(0) = 0$. We fit the function (4) to the experimental data by the method of least squares, varying all the parameters, i.e., D , T_N , and β . Since the width of the critical region is a priori unknown, in making this approximation we used various lower bounds on the interval of temperatures under study, with fixed upper bounds corresponding to loss of the NQR signal. This procedure should clearly test the stability of the parameter values obtained.

Figures 1 and 2 show the results of our approximations for the maximum range of temperatures 220–306 K (the solid lines). It is clear that there is good agreement between the experimental points and the power law (4). In Fig. 3 we plot the parameters D , T_N , and β obtained from our approximation versus the lower bound of the temperature interval. This figure reveals a slow decrease in the values we

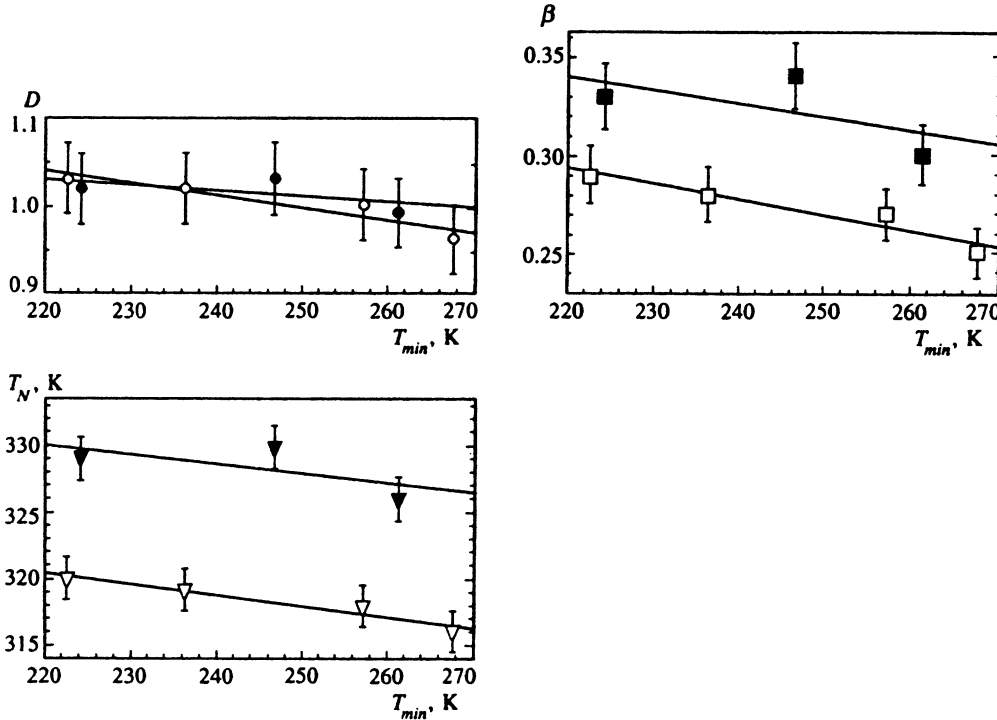


FIG. 3. Values of the parameters D , T_N , and β plotted versus the choice of a lower bound in approximating the temperature interval for normal (\circ , ∇ , \square) and high pressures (1.27 ± 0.07 GPa) (\bullet , \blacktriangledown , \blacksquare). The linear approximations are based on the method of least squares.

obtain both for the Néel temperature and the critical index of the magnetization as we approach the temperature T_k at which the second-order transition collapses. Since the high-temperature data should most correctly reflect the critical behavior of $\text{La}_2\text{CuO}_{4+\delta}$, we chose $T_N = 316$ K for the normal-pressure value of the extrapolated Néel temperature and $\beta = 0.26$ for the critical magnetization index.

The resulting pressure dependences of T_N and β were very stable, depending only slightly on the temperature interval used to make the approximations. From the data of Fig. 3 it follows that applying a pressure of 1.27 GPa causes the extrapolated Néel temperature to increase by (9.5–10.3) K, which corresponds to a positive baric coefficient $dT_N/dP = (7.8 \pm 0.5)$ K/GPa and relative coefficient $(1/T_N) \times (dT_N/dP) = 0.025 \pm 0.002$ GPa $^{-1}$. The critical index β increases significantly from 0.26 ± 0.02 at normal pressure to 0.31 ± 0.02 at high pressures. However, the change in the prefactor D of the power law (4) with pressure does not exceed measurement errors.

3. THEORY

Rather than turn immediately to a discussion of our results, we next derive a general expression for T_N that is correct for both the orthorhombic and tetragonal lattice phases.

A symmetry analysis of the magnetic structure of La_2CuO_4 , whose elementary magnetic cell is shown in Fig. 4, has been reported in a number of papers (see, e.g., Refs. 32–34). Using the results of these investigations, we can write the Hamiltonian of the system as a sum of two terms, one describing the intralayer interaction

$$\mathcal{H}_{\text{intra}} = \sum_n \left\{ \sum_{i=1,2} [J_{AF} S_{i\delta} S_{i\epsilon} - J_b S_{i\delta}^z S_{i\epsilon}^z - d(S_{i\delta}^y S_{i\epsilon}^z - S_{ib}^z S_{i\epsilon}^y)] \right\} \quad (5)$$

and the other the interlayer interaction

$$\mathcal{H}_{\text{inter}} = \sum_n \left\{ \sum_{\alpha \neq \beta = \delta, \epsilon} [(I+i/2) S_{1\alpha} S_{2\alpha} + (I-i/2) S_{1\alpha} S_{2\beta} - A(S_{1\alpha}^x S_{2\alpha}^x - S_{1\alpha}^y S_{2\alpha}^y) + A(S_{1\alpha}^x S_{2\beta}^x - S_{1\alpha}^y S_{2\beta}^y)] \right\}. \quad (6)$$

With the goal of consistently defining the parameters, we adhere to the notation of Ref. 25 and clearly identify contributions from individual cell (the expressions in curly brackets). In these expressions, indices $i=1,2$ label the CuO_2 layers, and $\alpha, \beta = \delta, \epsilon$ label the nearest neighbors within a layer. The parameter J_{AF} characterizes the intralayer antiferromagnetic exchange; due to the rhombic distortion the interlayer exchange interaction is determined by two parameters $J_{\epsilon\epsilon} = I+i/2$ and $J_{\delta\epsilon} = I-i/2$, where i is a small quantity reflecting the smallness of the rhombic distortion (see Fig. 4). The intralayer Dzyaloshinskii exchange-relativistic interaction d leads to noncollinearity of the magnetic moments in the CuO_2 layers. The anisotropic interactions J_b and A are also preserved in the tetragonal phase and probably are fundamental consequences of the relativistic interactions. Note that the anisotropy A of the interlayer forces is ignored in most papers. Nevertheless, as we will see below, its inclusion is decisive, for example, in generating a magnetically ordered state in the tetragonal phase of La_2CuO_4 .

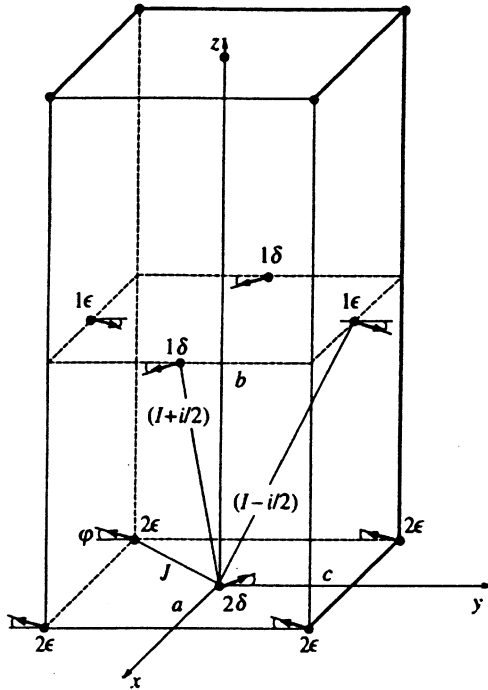


FIG. 4. Magnetic cell for La_2CuO_4 .

As is well known, the spin structure of La_2CuO_4 is that of a $4-x$ sublattice. In order to describe such a low-dimensional antiferromagnet it is necessary to introduce four magnetic sublattices.³⁵ However, as shown in Ref. 23, in the absence of an external magnetic field the system under study possesses a hidden symmetry. Namely, the Hamiltonian (5), (6) and the ground state (see Fig. 4) are invariant with respect to the operation

$$T_{\delta\delta}^{(12)}U_{2x}, T_{\delta\epsilon}^{(12)}U_{2y}, T_{\delta\epsilon}^{(ii)}U_{2z},$$

where $T_{\alpha\beta}^{(ij)}$ are translation operators between the corresponding atoms, while U_{2x} , U_{2y} , and U_{2z} are operators for a twofold-axis rotation of the spins relative to the x, y, and z axes. This allows us to reduce (5), (6) to a Hamiltonian for a system with a single atom per unit cell. The procedure used to carry out this transformation and the explicit form of the transformed Hamiltonian can be found in Ref. 23, and we will not give them here.

The expressions for the Néel temperature and the sublattice magnetizations are obtained by using the method of Green's functions³⁶ and the well-known identity that interrelates the operators $S_1^- S_1^+$ and S_1^z (as usual, $S_1^\pm = S_1^x \pm iS_1^y$). For the case of spin $S=1/2$, we obtain a simple relation between the correlation functions $\langle S_1^- S_1^+ \rangle$ and the average $\langle S_1^z \rangle$:

$$\langle S_1^- S_1^+ \rangle = \frac{1}{2} - \langle S_1^z \rangle. \quad (7)$$

It then follows from the spectral theorem for Green's functions that

$$\begin{aligned} \langle S_1^- S_1^+ \rangle &= \lim_{\delta \rightarrow 0} \pi^{-3} \int_0^\pi d\mathbf{k} \int_{-\infty}^\infty d\omega \\ &\times \frac{G^{-+}(\mathbf{k}, \omega + i\delta) - G^{-+}(\mathbf{k}, \omega - i\delta)}{\exp(\omega/T) - 1}, \end{aligned} \quad (8)$$

where $G^{-+}(\mathbf{k}, \omega)$ is the Fourier transform of the retarded Green's function³⁶

$$G^{-+}(\mathbf{l}-\mathbf{m}, t) = -i\theta(t)\langle [S_1^+(\mathbf{l}), S_m^-(0)] \rangle.$$

Note that the Green's function method gives the correct transition temperature of a quasi-two-dimensional magnet for the limiting values of the interplanar exchange interaction.^{37,38}

Formally, relations (7) and (8) allow us to find T_N exactly. The problem, however, is to compute the Green's function $G^{-+}(\mathbf{k}, \omega)$. Here we will make use of the equation-of-motion method, decoupling the chain of equations in the spirit of Bogolyubov and Tyablikov.³⁶ Doing so, we obtain a closed system of equations

$$\begin{aligned} (\omega - 2\langle S^z \rangle A_{\mathbf{k}})G^{-+}(\mathbf{k}, \omega) + 2\langle S^z \rangle B_{\mathbf{k}}G^{--}(\mathbf{k}, \omega) &= 2\langle S^z \rangle, \\ -2\langle S^z \rangle B_{\mathbf{k}}G^{-+}(\mathbf{k}, \omega) + (\omega + 2\langle S^z \rangle A_{\mathbf{k}})G^{--}(\mathbf{k}, \omega) &= 0, \end{aligned} \quad (9)$$

from which a new Green's function $G^-(\mathbf{l}-\mathbf{m}, t) = -i\theta(t)\langle [S_1^-(\mathbf{l}), S_m^-(0)] \rangle$ emerges. The coefficients $A_{\mathbf{k}}$ and $B_{\mathbf{k}}$ have the form

$$\begin{aligned} A_{\mathbf{k}} &= 2J_{AF} + 2i + 4A + 2d \sin(2\varphi) - [J_b \\ &\quad - d \sin(2\varphi)] \cos(ak_x) \cos(ck_y) - (A + 2I \\ &\quad - i) \cos(ck_y) \cos(bk_z) - A \cos(bk_z) \cos(ak_x), \\ B_{\mathbf{k}} &= -[2J_{AF} - J_b + d \sin(2\varphi)] \cos(ak_x) \cos(ck_y) \\ &\quad - A \cos(ck_y) \cos(bk_z) - (A - 2I \\ &\quad - i) \cos(bk_z) \cos(ak_x). \end{aligned}$$

Minimizing the energy of the ground state gives the value $\phi = d/2J_{AF}$ for the angle of noncollinearity.²³

By solving the system of equations (9) and substituting the value of $G^{-+}(\mathbf{k}, \omega)$ into (8) and (7), we obtain in the limit $\langle S_1^z \rangle \rightarrow 0$ an explicit relation for the Néel temperature:

$$T_N^{-1} = \frac{2}{N} \sum_{\mathbf{k}} \frac{A_{\mathbf{k}}}{A_{\mathbf{k}}^2 - B_{\mathbf{k}}^2}. \quad (10)$$

As is well known, the absolute value of the transition temperature obtained from (10) is an overestimate for two basic reasons. First of all, in deriving (10) we neglected the interaction of spin waves with each other. Secondly, the model does not take into account the effect of critical fluctuations, which exist in a narrow neighborhood of T_N . Nevertheless, the qualitative dependence of T_N on the system parameters is reliably given by Eq. (10), which we will use henceforth.

The integrals can be computed analytically only in a few limiting cases. Thus, in the isotropic model ($J_b = A = d = 0$) we have^{38,39}

$$T_N = \frac{\pi J_{AF}}{\ln(16J_{AF}/i)}. \quad (11)$$

In the tetragonal phase, inclusion of the intralayer anisotropy alone ($J_b \neq 0, A=d=i=1$) formally leads to a finite value of the ordering temperature. However, the orientations of the antiferromagnetism vectors of the CuO_2 layers in the plane ac are not correlated with one another, i.e., in reality there is no long-range magnetic ordering in the system. Inclusion of a weak interlayer anisotropy A ensures long-range magnetic order in the system even with $J_b=0$ (see Ref. 37). Thus, neglecting those terms in (10) that depend on the orthorhombic distortion ($i=d=0$), and also setting the anisotropy $J_b=0$ since it has only a weak influence on the transition temperature, we obtain the following expression for T_N in the tetragonal phase:

$$T_N = \frac{\pi J_{AF}}{\ln(16J_{AF}/A)}. \quad (12)$$

In general, an actual value of T_N can be obtained from Eq. (10) only numerically. We now turn to a discussion of the numerical results and compare them with the experimental data on the baric dependence of the Néel temperature in La_2CuO_4 .

4. DISCUSSION OF RESULTS

Within the framework of our model, the magnetic ordering temperature is a function of six parameters: the intralayer exchange J_{AF} , interlayer exchanges of rhombic i and tetragonal I origins; the Dzyaloshinskii interaction d ; and the anisotropies—the intralayer J_b and the interlayer A . At this time, uncertainties in the values of the main group of parameters (J_{AF}, i, d) have essentially been eliminated. We will use the results of the recent papers Refs. 23, 24, 40, and take as values for the normal-pressure state

$$\begin{aligned} J_{AF} &= 1490 \text{ K}, \quad I = 0.0 \text{ K}, \quad i = 0.02 \text{ K}, \\ J_b &= 0.04 \text{ K}, \quad d = 6.0 \text{ K}, \quad A = 0.01 \text{ K}, \end{aligned} \quad (13)$$

Since our intent is to establish qualitative regularities only, we have rounded off the values of the numbers in (13). As we have already noted, the interlayer anisotropy was not included in Ref. 25. Therefore, we started from the estimates of Refs. 23, 34, 40, which, however, we obtain using a somewhat different model than Ref. 25. (the choice of the parameter value I will be discussed below).

Figure 5 shows the results of our numerical calculation of the Néel temperature based on Eq. (10), plotted versus a single parameter with the other parameters fixed. The values of the latter were taken from the set (13) as starting values. The point 0 on this figure corresponds to the phase transition temperature T_N^0 at atmospheric pressure. As we might expect, T_N^0 greatly exceeds its experimental value.

Rather than compare the numerical results with experimental data, we simply note the following fact. A convenient structural parameter that correlates with the pressure is the angle the axis of the CuO_6 octahedron makes with the b axis of the crystal. At room temperature this angle decreases smoothly from a value of $\approx 4.5^\circ$ at zero external pressure to zero at the critical pressure $P_c = 3.6 \text{ GPa}$ where the orthorhombic-to-tetragonal structural transition occurs. This value of P_c is comparable to our maximum pressure. Thus,

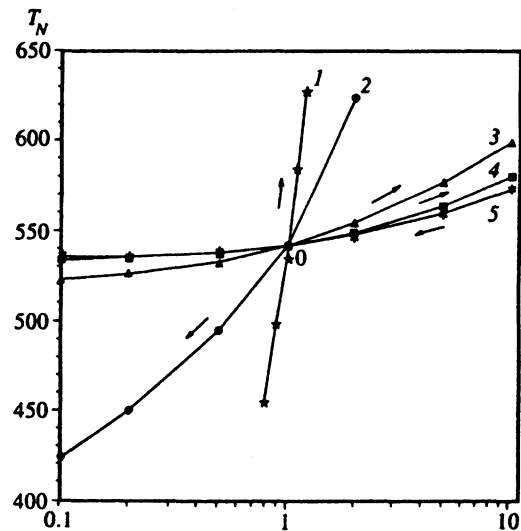


FIG. 5. Dependence of the Néel temperature on one of the magnetic parameters of the system with the remaining parameters fixed, according to numerical calculations based on Eq. (10). The direction of change of the system parameters with increasing pressure is shown by arrows. The point of intersection of all the curves corresponds to a magnetic ordering temperature at atmospheric pressure. Along the abscissa (logarithmic scale) we plot the relative values of the system parameters, also on a logarithmic scale: $1 - J_{AF}/J_{AF}^0$, $2 - d/d^0$, $3 - J_b/J_b^0$, $4 - A/A^0$, $5 - i/i^0$; J_{AF}^0 , d^0 , J_b^0 , A^0 , i^0 are variables at normal pressure (13).

by knowing the characteristics of the change in the lattice, we can with a high degree of reliability infer the direction of change of the system magnetic parameters relative to their original values (13). In Fig. 5 we use arrows to indicate the direction of change of the magnetic parameters under pressure.

Comparison of the experimental data with the numerical analysis leads to the following qualitative conclusions.

1. The isotropic model predicts the pressure dependence of the Néel temperature incorrectly. In order to make (11) agree with experiment, we must increase the value of the uncompensated interlayer exchange by a factor of 1.5 to 3. This is contradicted by the decrease in the rhombic distortion and the corresponding decrease in the parameter i as the pressure increases.

2. The variation in the intralayer exchange interaction J_{AF} under pressure (according to Ref. 41, $(1/J_{AF}) \times (dJ_{AF}/dP) = 0.013 \text{ GPa}^{-1}$) can explain only about 50% of our data for $(1/T_N)(dT_N/dP)$, and only 20% if we compare with the results of Ref. 13.

3. The effect of the tetragonal part of the interlayer exchange I on T_N is extremely small (we do not show the function $T_N(I)$ in Fig. 5). Varying I from zero to $0.1J_{AF}$ changes T_N by no more than 3 K, which is below the precision of our numerical methods. This implies that although the exchange I can also be rather large, the total molecular field exerted by the spins of the upper and lower planes on a Cu^{2+} ion is almost completely compensated.

4. The rhombic Dzyaloshinskii interaction decreases with increasing pressure. Our numerical results show (see Fig. 5) that the decrease in d leads to a sharp dropoff in

T_N , which once more is contradicted by the experimental dependence $T_N(P)$.

The facts listed above show the important role of the anisotropic interactions in creating the magnetic properties of La_2CuO_4 .

5. The required direction of change of the ordering temperature can be ensured by the most likely increase in the intralayer anisotropy J_b with pressure. However, in order to match the experimental increase in T_N it must vary by a rather large amount—about 25% of the original value at 1.3 GPa. Since the basic structural element of a layer is a rather “rigid” almost square lattice made up of Cu–O bonds, this requires some additional justification.

6. We have observed that interlayer anisotropy plays a rather important role in creating the critical magnetic properties of La_2CuO_4 . First of all, as we have already noted, it leads to a finite magnetic ordering transition temperature even when the lattice (12) is tetragonal. Secondly, the quantitative contribution of this type of anisotropy to T_N is consistent with the contribution of the ordinary intralayer anisotropy J_b .

It is clear that as the pressure increases all the parameters of the system vary simultaneously. Therefore, since they must not only compensate the decrease in T_N due to decreasing rhombic character of the crystal but also generate a net increase in the ordering temperature, the anisotropic interactions must be even more important than our analysis of the data shown in Fig. 5 implies.

As for the critical index β (see Fig. 2), its value of 0.26 at atmospheric pressure implies that La_2CuO_4 shows no sign of the vortex phase transition that is characteristic of a planar degenerate system with $\beta=1/8$.⁴² The increase of the value of β to 0.31 with increasing pressure reflects a tendency toward enhancing the interlayer interactions. Nevertheless, the quasi-two-dimensional properties of La_2CuO_4 are still preserved, because $\beta < 1/3$.

5. CONCLUSION

In light of the conclusions we have arrived at, let us briefly discuss the results of previous papers.

The difficulties in interpreting resonance measurements of the Néel temperature in La_2CuO_4 mentioned in Sec. 2 clearly illustrate the reasons for the large methodological difficulties that arise when nonlocal methods are used. In those investigations at normal and high pressures where T_N was identified with the temperature at which electrical conductivity anomalies occur,^{10–12,43,44} it is probable that the first-order phase transition temperature T_k was recorded, at which a jump occurs in the sublattice magnetization of $\sim(0.3–0.4)M(0)$. In our view, one indication of this is the fact that the decrease in electrical conductivity below the magnetic ordering temperature revealed by single-crystal measurements¹² is found to be much larger than the decrease expected from scattering of carriers at a second-order antiferromagnetic transition.¹¹ It is also unsurprising that a negative sign was obtained in Refs. 10–12, 44 for the baric coefficient of the magnetic ordering temperature. This correlates with our data, which show a decrease in T_k with increasing pressure. Moreover, we are in satisfactory quanti-

tative agreement with the data of Ref. 12, which is based on the position of the electrical conductivity maximum and which predicts a value $((dT_k/dP)\approx -2.5 \text{ K/GPa})$ for a single crystal sample. At the same time, in Refs. 10, 11, where the position of the minimum in the temperature derivative of the electrical resistivity dR/dT was investigated in polycrystals, the authors report a negative baric coefficient for the ordering temperature with a much larger modulus of $-(5–10) \text{ K/GPa}$, while in Ref. 43 a positive value was obtained for (dT_N/dP) . These discrepancies could arise, for example, when nonuniformity of the applied pressure extends the range over which the transition is washed out (i.e., the regions of coexisting phases).

Also unsurprising is the situation when the magnetic ordering temperature for order-disorder is identified with the position of the maximum in the magnetic susceptibility $\chi(T)$. According to the data of Ref. 14, the position of this maximum approximately corresponds to the center of the heterogeneous region, i.e., where the first-order transition temperature is referenced from a level of 0.5 of the temperature dependence of the volume of antiferromagnetic phase. The true anomaly (maximum) of $\chi(T)$ at the Néel point, which would occur if a second order transition took place, is found to be “cut off” on the high-temperature side as a result of the almost discontinuous decrease in the volume of the antiferromagnetic phase. In our view, this is the reason why the authors of Ref. 10 obtained a negative baric coefficient of order -5 K/GPa from their measurements of the susceptibility.

Finally let us discuss the results of neutron scattering studies reported in Ref. 13, which differ markedly from all the other data. In Ref. 13 the magnetic ordering point was identified with a break in the temperature dependence of the (100) magnetic reflection. Although this break is only weakly expressed against a large background reflection, the authors succeeded in recovering a baric dependence of the magnetic ordering temperature with a very large slope $(dT_N/dP)=18.5\pm 0.15 \text{ K/GPa}$ or $(1/T_N)(dT_N/dP)=0.083 \text{ GPa}^{-1}$. Thus, this paper, like ours, reports a positive baric coefficient for the magnetic ordering temperature. However, their relative coefficient exceeds ours by almost a factor of 3. Since neutron scattering investigations of this break should, like the other techniques, measure the temperature T_k for the first-order phase transition, the positive sign of the baric coefficient remains ambiguous. We can postulate several reasons for this phenomenon. Thus, the sample used in Ref. 13 had a very low value of the magnetic ordering temperature $\sim 220 \text{ K}$, implying a large concentration of excess oxygen and, accordingly, of holes. We cannot ignore the possibility that, as a result, the collapse of the second-order transition to a first-order transition, which is characteristic of stoichiometric insulating samples, does not occur in this system. In that case, the authors of Ref. 13 measured the true rate of change of the Néel temperature T_N with pressure, but for a sample in which the dominant contribution comes from competing exchange interactions.¹⁸

A final comment should be made with regard to models that relate the behavior of the Néel temperature of a base material under pressure to the critical temperature for the

superconducting transition in a corresponding superconducting version of this material (see, for example, Ref. 43). Because the baric behavior of T_N is to a considerable degree due not only to exchange but also magnetic relativistic interactions, effects that are not included in these models, the justification of the latter remains very problematic.

Thus, in this paper we have used NQR of ^{139}La to precisely recover the dependence of the critical magnetic properties of La_2CuO_4 on pressure. Our values for T_N were obtained by extrapolating the temperature dependences of $H_{\text{loc}}(T)/H_{\text{loc}}(0) \sim M(T)/M(0)$ to zero. We have established that the Néel temperature increases with pressure at a rate of $(dT_N/dP) = 7.8 \text{ K/GPa}$. When the change in the structure of the La_2CuO_4 lattice is taken into account, this implies that the magnetic ordering temperature of the copper Cu^{2+} ions in the rhombic phase increases as the angle of deviation of the CuO_6 octahedron decreases. Comparison of theoretical calculations with the results of experiment indicate a considerable role for anisotropic interactions in generating the magnetic properties of La_2CuO_4 .

¹⁾An alternative point of view held by the authors of Ref. 12 is that the cause of this strong scattering is strong coupling of charge carriers to localized magnetic moments.

¹Yu. A. Izyumov, N. M. Plakida, and Yu. N. Skryabin, Usp. Fiz. Nauk **159**, 621 (1989) [Sov. Phys. Usp. **32**, 1060 (1989)].

²Yu. A. Izyumov, Usp. Fiz. Nauk **161**, 1 (1991) [Sov. Phys. Usp. **33**, 313 (1991)].

³A. P. Kampf, Phys. Rep. **249**, 219 (1994).

⁴I. Felner and I. Nowik, Supercond. Sci. Technol. **8**, 121 (1995).

⁵H. Takahashi, H. Shaked, B. A. Hunter, et al., Phys. Rev. B **50**, 3221 (1994).

⁶R. Moret, J. P. Pouget, C. Noguera, and J. Collins, Physica C **153–155**, 968 (1988).

⁷H. J. Kim and R. Moret, Physica C **156**, 363 (1988).

⁸C. J. Howard, R. J. Nelmes, and C. Vettier, Solid State Commun. **69**, 261 (1989).

⁹H. Takahashi and N. Mori, in *Studies of High-Temperature Superconductors*, Vol. 16, p. 1, A. V. Narlikar (ed.), Nova Science Publishers, New York (1995).

¹⁰B. Barbara, J. Beille, A. Draperi, et al., J. de Physique **49**, C8-2139 (1988).

¹¹J. Beille, J. Demazeau, H. Dupendant, et al., Physica C **157**, 446 (1989).

¹²M. C. Aronson, S.-W. Cheong, F. H. Jarzon, et al., Phys. Rev. B **39**, 11445 (1989).

¹³S. Katano, N. Mori, H. Takahashi, and H. Takei, J. Phys. Soc. Jpn. **58**, 3890 (1989).

¹⁴V. A. Borodin, V. D. Doroshev, Yu. M. Ivanchenko et al., JETP Lett. **52**, 469 (1990).

¹⁵Yu. M. Ivanchenko and A. E. Filippov, and A. V. Radievskii, Fiz. Nizk. Temp. **19**, 655 (1993) [Low Temp. Phys. **19**, 468 (1993)].

¹⁶H. Tang, J. Xiao, A. Sing, et al., J. Appl. Phys. **67**, 4518 (1990).

¹⁷M. F. Hundley, J. D. Thompson, S.-W. Cheong et al., Phys. Rev. B **41**, 4062 (1990).

¹⁸A. Aharony, R. J. Birgeneau, A. Coniglio et al., Phys. Rev. Lett. **60**, 1330 (1988).

¹⁹H. Nishihara, H. Yatsuoka, T. Shimizu et al., J. Phys. Soc. Jpn. **56**, 4559 (1987).

²⁰H. Lütgemier and M. W. Pieper, Solid State Commun. **64**, 267 (1987).

²¹I. Firo and A. Janossy, Jpn. J. Appl. Phys. **25**, L1307 (1987).

²²V. A. Borodin, V. D. Doroshev, S. F. Ivanov et al., Fiz. Tverd. Tela **36**, 1699 (1991) [Sov. Phys. Solid State **36**, 956 (1991)].

²³V. D. Doroshev, V. N. Krivoruchko, M. M. Savosta et al., Zh. Eksp. Teor. Fiz. **101**, 190 (1992) [Sov. Phys. JETP **74**, 102 (1992)].

²⁴V. V. Babenko, V. G. But'ko, A. A. Bush et al., Fiz. Tverd. Tela **36**, 241 (1994) [Phys. Solid State **36**, 131 (1994)].

²⁵J. Berger and A. Aharony, Phys. Rev. B **46**, 6477 (1992).

²⁶T. Tsuda, T. Shimizu, H. Yatsuoka et al., J. Phys. Soc. Jpn. **57**, 2908 (1988).

²⁷N. E. Aibinder, Fiz. Tverd. Tela **31**, 240 (1989) [Sov. Phys. Solid State **31**, 683 (1989)].

²⁸T. C. Wang, Phys. Rev. **99**, 566 (1955).

²⁹V. D. Doroshev and M. M. Savosta, JETP Lett. **50**, 363 (1989).

³⁰A. Abragam, *The Principles of Nuclear Magnetism*, Clarendon Press, Oxford (1961).

³¹V. A. Borodin, V. D. Doroshev, S. F. Ivanov et al., preprint No. 89-425, Donets Physico-Mechanical Institute, National Academy of Sciences of Ukraine (1989).

³²A. S. Borovik-Romanov, A. I. Buzdin, N. M. Krein's, and S. S. Krotov, JETP Lett. **47**, 697 (1988).

³³B. G. Bar'yakhtar, V. M. Loktev, and D. A. Yablonskii, Physica C **156**, 667 (1988).

³⁴Yu. G. Pashkevich, V. V. Shakhov, V. A. Blinkin et al., Fiz. Nizk. Temp. **20**, 423 (1994) [Low Temp. Phys. **20**, 335 (1994)].

³⁵A. I. Zvyagin, M. I. Kobets, V. N. Krivoruchko et al., Zh. Eksp. Teor. Fiz. **89**, 2298 (1985) [Sov. Phys. JETP **62**, 1328 (1985)].

³⁶V. N. Zubarev, Usp. Fiz. Nauk **71**, 71 (1960) [Sov. Phys. Usp. **3**, 320 (1960)].

³⁷M. E. Lines, Phys. Rev. **131**, 540 (1963).

³⁸M. E. Lines, Phys. Rev. **135**, A1336 (1964).

³⁹A. Du, Z. Wei, Q. L. Hu, and Z. Xianyin, Int. Conf. Magn. ICM94, 22–26 August, 1994, Warsaw, Wydawn. Nauk. Abstrakts, p. 35.

⁴⁰V. N. Krivoruchko and T. E. Primak, Fiz. Nizk. Temp. **19**, 871 (1993) [Low Temp. Phys. **19**, 620 (1993)].

⁴¹M. C. Aronson, S. B. Dierker, B. S. Dennis et al., Phys. Rev. B **44**, 4657 (1991).

⁴²A. Z. Patashinskii and V. L. Pokrovskii, *Fluctuation Theory of Phase Transitions* [in Russian], Nauka, Moscow (1982) [Pergamon Press, Oxford (1979)].

⁴³T. Kaneko, H. Yoshida, Y. Syono et al., Physica B **148**, 494 (1987).

⁴⁴M. Kurisu, S. Matsuda, T. Suzuki, and T. Fujita, Physica C **179**, 358 (1991).

Translated by Frank J. Crowne